Icarus 206 (2010) 164–173

Contents lists available at ScienceDirect

Icarus

journal homepage: www.elsevier.com/locate/icarus

The loss of water from Mars: Numerical results and challenges

Stephen H. Brecht [a,*], Stephen A. Ledvina [b]

[a] Bay Area Research Corp., Orinda, CA 94563, USA
[b] Space Sciences Laboratory, Univ. of California, Berkeley, CA 94720, USA

ARTICLE INFO

Article history:
Received 12 October 2008
Revised 27 April 2009
Accepted 30 April 2009
Available online 23 May 2009

Keywords:
Mars
Ionospheres
Solar wind

ABSTRACT

The simulation of Mars is a very challenging effort. However, simulations are a major method of addressing the issues of the solar wind interaction with Mars. Further, it is via simulations that issues such as water loss from Mars via solar wind pick up of ionospheric ions will be addressed. This paper discusses some of the issues raised during the Chapman Conference on Solar Wind Interactions with Mars, SWIM. It also addresses numerical issues and the authors attempts to address them, coupled with results of preliminary simulations of Mars.

1. Introduction

Of all of the objects in the solar system Mars offers perhaps the most challenging set of conditions to simulate. The numerical challenges come from the following facts: (1) The solar wind interacts directly with the ionosphere of the planet. (2) The fact that the shock stands-off from the surface of the planet less than a proton gyroradius. (3) The planet is small, and there are crustal fields on the surface of the planet possessing fields as much as 300 times as intense as the solar wind IMF. Yet these fields are distributed about the surface of the planet in a very inhomogeneous manner.

These challenges mean that a simulation must address the kinetic behavior of the interaction, and include the physics that forms the shock self-consistently. Items one through three mean that the chemistry of the ionosphere must be included, and that multiple ion species must be tracked because the ionospheric is not comprised of protons. One should also consider the ion–neutral interactions. Adding more complexity is the planetary boundary condition. Does one assume it is a conductor? Does one assume it is electromagnetically absorbing? How does one handle the crustal fields, resolve them, and address the enormous increase in ion gyrofrequency of the ions in such strong local magnetic fields?

These challenges (chemical, physical, numerical) are befitting the most accomplished simulation groups in the world. And indeed many researchers have performed simulations of Mars using different approaches and assumptions. A brief discussion of these different approaches are discussed in a paper from this issue (Brain et al., submitted for publication). Further, these simulations are evolving as each groups gains better insight into their simulation codes capabilities, weaknesses, and needs. Needless to say, each groups addresses the list of challenges mentioned above from a different point of view. In light of this concerted effort, a Chapman conference was held to make a first attempt at comparing the codes, their results and their weaknesses (Brain et al., submitted for publication).

The motivation for these efforts is driven by missions to Mars for example Phobos-2, the current mission Mars Express, and of course Mars Global Observer, MGS. It was MGS that discovered the crustal fields of Mars, a truly unique feature in all of the solar system (Acuna et al., 1998). It was MGS that provided the largest data sets to date with regard to magnetic fields, and plasmas. However, MGS did not have all of the instruments needs. The European Space Agency, ESA, spacecraft, Mars Express as been filling the gap with regard to plasma data, but carries no magnetometer. Beyond the questions driven by the amazing data collected by these spacecraft and others, there is a deeper issue being addressed or being staged to be addressed by these simulation groups and it is connected to the search for possible life on other planets. That is the issue of water on Mars and where it might have gone.

1.1. Overview of the major issue

The missions to Mars clearly indicate that the solar wind interacts directly with the atmosphere/exosphere/ionosphere of these planets. This interaction results in the loss of ions from Mars. Numerical simulations have been undertaken to make an estimate of these losses. The current understanding of the solar wind interaction with Mars has been reviewed by Mazelle et al. (2004) and Nagy et al. (2004).

The Phoenix Mars Lander has confirmed what has been a source of speculation for sometime. Mars has water or at least some water. The issue remains what happened to the surface water.

* Corresponding author.
E-mail address: sbrecht@pacbell.net (S.H. Brecht).

0019-1035/$ - see front matter © 2009 Elsevier Inc. All rights reserved.
doi:10.1016/j.icarus.2009.04.028

There are a variety of possibilities. One of those possibilities is the focus of the research in this paper: water loss via ion pickup by the solar wind.

There are a variety of theories concerning the amount of water present on Mars during earlier epochs and where it may have gone (cf. Lammer et al., 1996). One of the more complete papers concerning this topic is by Lammer et al. (2003). In this paper the authors discuss the various mechanisms for water loss and the issue of water being tied up in the soil. One of the major loss mechanisms proposed is that of pick up of oxygen ions via the solar wind interaction with the Martian ionosphere/exosphere. Fox (1997) produced an estimate of what it would take to achieve the 2:1 ratio of hydrogen to oxygen for water loss. In her estimate the rate needed to be roughly 1×10^{26} oxygen atoms per second or roughly 1.2×10^{8} cm^{-2} s^{-1} in today's Martian environment. It is worth noting that a loss rate of 10^{26} oxygen ions per second would remove a meter of water from the entire surface of Mars in 1.72 Gy.

Data from Phobos-2, which orbited Mars during the solar maximum period, indicate a loss rate of 3×10^{25} ions s^{-1} (Lundin et al., 1989, 1990). The Mars Express data taken at solar minimum conditions indicate ion loss rates on the order of 3×10^{24} (Lundin et al., 2008). However, even within the Mars Express research community there is considerable variations in the estimated loss rate. Newer numbers are becoming available as better algorithms allow analysis of instrument data at lower energies.

In the winter of 2008 a Chapman Conference was held addressing the issue of Mars and its interaction with the solar wind. Included in this conference was the first round of comparisons between seven major groups of numerical simulators (Brain et al., submitted for publication). The results of the simulations were compared to specified orbits from Mars Express. The comparisons presented an eye opening challenge to all concerned.

Calculating moments of the data was not trivial, and many assumptions were required. Pressure was one quantity to be compared. This provided a challenge to both experimentalists and simulation groups. The pressure is not isotropic especially in the subsolar regions near the shock. Another quantity to be compared was the planetary ion loss rates. For the spacecraft data this quantity was not trivial to estimate, due to energy resolution limitations on the spacecraft instruments, large ion gyro-orbits of pick up ions such as oxygen coupled with the possibility that the distributions were not isotropic, and finally because one has to assume the orbit sampled a representative pick up ion density, when all simulations and most spacecraft data clearly show that Mars presents probably one of the most asymmetric plasma environments in the solar system. That statement holds true without the presence of the crustal fields in the simulations. Therefore, it becomes essential to understand the "error" bars within the data and the simulations.

The simulations also produced interesting results with variations of over a factor of 20 in the ion pickup rate of O^+ (Brain et al., submitted for publication). However, many of the simulations were close to one another but this agreement did not organize itself with regard to numerical scheme. For example the results of Brecht and Ledvina were reasonably close to MHD simulations by Ma et al. (see Brain et al., submitted for publication). What was similar is that both groups used the same chemistry equations to create and maintain their ionospheres (cf. Ma et al., 2004; Brecht and Ledvina, 2006). Other hybrid simulations produced lower pick up rates. The good news was that ion pickup rates where very close to those reported from Phobos-2 during solar maximum (Brecht and Ledvina, 2006). Further, both Ma et al. (Brain et al., submitted for publication) and our group predicted loss rates that were very close to those measured by MEX during the solar minimum. The bad news, the simulations reported in this paper and earlier work did not include crustal fields and need to be run with better resolution.

This leaves one with several issues to address both from a numerical standpoint and a physics standpoint. From a numerical standpoint how much is enough to make good predictions. That question cannot be answered yet, but with further code comparisons the answer may be forthcoming. From a physics/chemistry standpoint, is it really true that all one has to do is place the appropriate ionospheric chemistry into the codes to obtain the "correct" answer? Not likely as another MHD group also had a complex chemistry suite in their code and their results differed from Ma et al. and Brecht and Ledvina. However, the issue of how important the ionospheric boundary is to the results is a crucial question that further code comparisons can address. The role of the crustal fields is a major topic to address and will be discussed later in this paper. Finally, it is clear one cannot establish the validity of the results by comparing to one global number even if that number is very important to establishing the history of water on Mars. The problem is simply too complex. The code comparison has led the authors of this paper to suggest that a different form of comparison is really required. This will also be discussed in this paper.

The purpose of this paper is not to present definitive answers to some of the fundamental questions associated with the Martian interaction with the solar wind. Rather, it is to illustrate parametric sensitivities both of the numerical and physical nature. This paper presents the results of our contributions to the code comparison at the Chapman conference, and the continuing efforts to improve the simulations as well as understand the sensitivities of the solar wind interaction with Mars. To accomplish this several examples of simulation sensitivity studies will be presented, very preliminary parameter studies will be discussed, and a discussion of the results and what they mean to future simulations of Mars will be presented. In the following paragraphs, the simulation numerics and conditions will be presented and discussed, followed by some of the simulation results, and then issues of sensitivity and future research will be discussed.

2. Numerical code

To estimate the global loss of oxygen from Mars scientists have employed two distinct numerical approaches to make these estimates. One is the MHD formalism (cf. Liu et al., 2001; Ma et al., 2002, 2004; Harnett and Winglee, 2006) and the second is the kinetic formalism, specifically the hybrid particle code (Kallio and Janhunen, 2002; Bößwetter et al., 2004; Modolo et al., 2005). See Ledvina et al. (2008) for a further discussion of all of these schemes. Most if not all of the results to date have produced O^+ and O_2^+ loss rates that are consistent or less than those measured by the ASPERA instrument on Phobos-2 and MEX (Brain et al., submitted for publication).

The research presented in this paper employs hybrid particle simulations using the HALFSHEL code. The HALFSHEL code has been used in simulations of unmagnetized bodies for many years (cf. Brecht, 1990; Brecht and Ferrante, 1991; Brecht et al., 1993a; Brecht, 1995a,b; Brecht, 1997a,b; Brecht et al., 2000; Ledvina et al., 2004). However, the current version of the code has had some additional physics added to it. The code currently has an extensive set of ionospheric chemistry equations within it to produce and maintain the ionosphere (see Table 1). Because of the low altitude of the ion pickup a conductivity tensor model was placed in the code and will be briefly discussed in the next paragraphs. This tensor provides both Hall and Pedersen conductivities in the regions where ion–neutral and electron–neutral collisions are important.

The hybrid model treats all ion species (the model can carry as many as one wishes) as kinetic particles and thus are advanced with a simple Lorentz force equation. The electrons are treated as

use for initial implementation of chemistry

www.issibern.ch/teams/martianplasma/

Table 1
Chemical reactions for simulations.

1.	$O + h\nu \rightarrow O^+ + e$	$k = 2.73 \times 10^{-7}$ s^{-1}
2.	$CO_2 + h\nu \rightarrow CO_2^+ + e$	$k = 7.3 \times 10^{-7}$ s^{-1}
3.	$O + e \rightarrow O^+ + e + e$	k, Cravens et al. (1987)
4.	$CO_2^+ + O \rightarrow O_2^+ + CO$	$k = 1.64 \times 10^{-10}$ cm^3/s
5.	$CO_2^+ + O \rightarrow O^+ + CO_2$	$k = 9.6 \times 10^{-11}$ cm^3/s
6.	$O^+ + CO_2 \rightarrow O_2^+ + CO$	$k = 1.1 \times 10^{-9}$ cm^3/s
7.	$O^+ + e \rightarrow O$	$k = 3.2 \times 10^{-12}$ cm^3/s $(250/T_e\ (K))^{0.7}$ cm^3 s^{-1}
8.	$O_2^+ + e \rightarrow O + O$	$k = 7.38 \times 10^{-8}$ cm^3/s
9.	$CO_2^+ + e \rightarrow CO + O$	$k = 3.1 \times 10^{-7}$ cm^3/s

No hydrogen at all: why?

a massless fluid. Therefore, electromagnetic waves up to and including the whistler are carried in the code. Shock formation is included in the physics of this code and thus needs no assumptions or numerical techniques to capture the shock. The basic equations of the hybrid model are well known and need not be repeated here. See Ledvina et al. (2008), Brecht and Ledvina (2006), Brecht and Thomas (1988), and Harned (1982) for a more complete discussion. However, it is worth noting a few of the models that have been added to the basic hybrid code. One is an expansion of the electric field model. The basic electric field equation comes from the inertialess electron momentum equation

$$0 = -en_e\boldsymbol{E} + \boldsymbol{J}_e \times \boldsymbol{B}/c - \nabla p_e + en_e\eta\boldsymbol{J}$$

where the resistivity, η, is usually just a numerical factor, $\boldsymbol{J}_e$ is the electron current, and p_e is the electron pressure. In the current hybrid model the electric field equation is expanded to include both Hall and Pedersen conductivities, thus creating much more complex current patterns in regions where collisions are a significant factor. The generalized electric field (Mitchner and Kruger, 1973) is

$$\boldsymbol{E} = \frac{\boldsymbol{J} + \beta_e\boldsymbol{J} \times \boldsymbol{B} + s\boldsymbol{B} \times (\boldsymbol{J} \times \boldsymbol{B})}{\sigma} - \frac{1}{en_e}\nabla p_e$$

where the σ is the conductivity, $\boldsymbol{J}$ is the total current density, β_e is the electron Hall parameter, (ω_{en}/ν_{eH}) with $\omega_{en} = eB/m_e$, the electron cyclotron frequency, and ν_{eH} is the electron collision frequency (electron–neutral and electron–ion). $\boldsymbol{B}$ is the magnetic field and the ion slip factor, s, is $((\rho_n/\rho)^2\beta_e\beta_i)$ where ρ_n is the neutral density, ρ is the total density (ion + neutral), and β_i is the ion Hall parameter (ω_{in}/ν_{in}). In the limit that the collision frequencies go to zero, this equation returns to the normal electric field equation found in a hybrid particle code, where the electron current is needed, as well as the electron pressure gradient (Brecht and Thomas, 1988). The electron–ion collision frequencies were taken from Mitchner and Kruger (1973). The electron–oxygen (neutral) and electron–CO_2 (neutral) collision frequencies were taken from Strangeway (1996).

Rather than loading an ionospheric profile or simply injecting the ionospheric plasma as is done by some modelers, it was found to be more accurate to actually solve the chemistry equations. Table 1 contains the list of the reactions currently solved in the Mars simulations. The electron temperature necessary for reactions such as impact ionization is set to a predetermined value (Shinagawa and Cravens, 1989) for altitudes below 500 km. This was done because the code does not contain electron heat convection, nor the complete reaction set to properly predict the electron temperature at these low altitudes. Above 500 km, the electron temperature is calculated by solving the energy equation for electron temperature (cf. Brecht and Ledvina, 2006).

3. Results

The simulations to be discussed are derivative of our standard simulation set of parameters. The SWIM simulation used essentially the same set of parameters with the only changes being in the EUV flux and the neutral atmosphere profile which were provided by the organizers of the meeting. The following table shows those parameters, Table 2. The nominal or standard run was for solar maximum consistent with the conditions when Phobos-2 was orbiting Mars. All other simulations used these same parameters with only the EUV flux and/or the neutral profile being changed.

4. Loss rates

As we continued to test and improve the chemistry we also improved our ability to handle the neutrals in the chemistry, and are now capable of including 3D neutral models from atmospheric simulations. One of the other aspects of our present effort was to further explore the non-linearity of the ion pickup rates as a function of simple parameters.

The paper published by Brecht and Ledvina (2006) examined sensitivities of the ion pick up rate as a function of physical and numerical parameters. The focus at the time was solar maximum conditions consistent with the Phobos-2 data. The results were high but consistent with Phobos-2 data (Lundin et al., 1989, 1990). However, the simulations displayed how sensitive the result could be based on some simple changes in the input parameters. For example, for most of the simulations we used a 1D neutral density profile as provided and used by Nagy and his group. When a solar zenith angle dependent cosine taper was added to the neutral density profile with the nightside having a smaller scale height, the pickup rate dropped by roughly 50%. That simple change made a rather substantial difference. We also examined the pickup rate if we simply changed the EUV flux from solar maximum values to three times and six times this value. The loss rates increased to above 10^{26} O^+/s but did not increase linearly.

Table 3 shows the oxygen ion loss rate as we vary the EUV flux while keeping solar wind and neutral profiles constant. One sees that the pickup rates do not change linearly with increased EUV frequency. This table as well as other simulations and the comparison efforts performed for the Jan. 2008 Chapman conference on Solar Wind Interaction with Mars, suggest a different tactic in simulations efforts. It suggests that rather than trying to match estimated numbers from the data, we use the data as a guideline to indicate if we are in the realm of reason but take it a step further.

The step further is to perform many simulations and examine scaling of the results and then compare the scaling with such data as exists, for example the solar maximum and solar minimum results returned by Phobos-2 and MEX. It is our contention that matching scaling from the code to scaling from the data will be more productive and indicative of having the correct physics or sufficient physics in the simulations. Perhaps just as importantly, comparisons with other simulation groups will be more productive as one can see which codes are more sensitive to various parameters, thus offering insight into how the real situation surrounding Mars may well respond to the solar wind. Finally with scaling rela-

Table 2
Simulation conditions.

Solar conditions	Maximum	SWIM
B magnitude (nT)	3	3
B_x	0.83 * B	0.83 * B
B_y	0.0 * B	0.0 * B
B_z	0.56 * B	0.56 * B
Density (cm^{-3})	2	2
T_e (eV)	17	17
T_i (eV)	1.0×10^{-11}	1.0×10^{-11}
Velocity (km/s)	425	425
EUV frequency (s^{-1})	2.73×10^{-7}	8.89×10^{-8}

Table 3
EUV fluxes vs. oxygen ion loss rates.

EUV frequency (s^{-1})	Oxygen ion loss rate #/s
8.890×10^{-8} Solar min.	8.0×10^{24}
2.730×10^{-7} Solar max.	5.2×10^{25}
8.190×10^{-7} 3× Solar max.	3.1×10^{26}
1.638×10^{-6} 6× Solar max.	3.6×10^{26}

tions researchers making estimates of losses from earlier epochs can more easily assess the assorted assumptions often made for these periods with regard to the role of ion pickup in the loss of water from Mars as well as the evolution of the atmosphere.

Fig. 1 shows the EUV frequency plotted against the oxygen loss rates (solid line). One sees that up until the 6 times normal situation the loss rate is an exponential curve and a very straight one at that. Fitting this data is illustrated by the dashed line in Fig. 1. The attempt at fitting was crude and with four points not very accurate. Nevertheless, one sees a clear functional dependence is a logarithmic function rather than linear. Such information, if extended to cover the range of potential EUV frequencies consistent with early Martian and solar epochs to the present day, could be used to evaluate the loss rates. However, other parameters must be included as well. We believe that by developing these scaling functions a better comparison can be made with other simulation codes and to data.

The issue of earlier epochs is rather complex. It was already shown that the pickup rate did not scale linearly with increases with the ionization frequency, Fig. 1. One can speculate that as the EUV flux went up self-shielding of the system occurred as the ions were being picked up. Since the same neutral density was used and was not modified, "burn out" of the upper ionosphere via depletion of the neutrals was not possible. This leads to interesting issues with regard to the lower ionosphere/atmosphere. If the upper boundary is losing ions at an ever increasing rate, as one might expect during earlier epochs where the atmosphere of Mars was more extensive and the solar wind stronger with regard to fields and speed, at what rate can the lower ionosphere/atmosphere supply more neutrals? Further, if the atmosphere/ionosphere is more extensive does this protect the lower regions from the applied convection electric field? In the case of Venus the stronger well formed shock does protect Venus and the ion loss rates are not much different than from Mars. The best we can do is supply a loss rate for the upper boundary condition that scientists more knowledgeable about Mars' atmosphere can use. However, the issue of water loss will be affected by the rate at which water vapor can leave the surface, be transported to the upper ionosphere (the altitude for peak ion pickup is found both experimentally, MEX, and via simulation to between 250 and 300 km) and then be subjected to the solar wind pickup fields.

5. Parallel electric fields

During the last few years our efforts have been focused on a variety of issues discovered as we continued to improve the simulations capabilities. One of the improvements was to address the accuracy of our chemistry package. Chemistry is not easy to do in a particle code and it required a bit of a learning curve to implement it in an accurate fashion (Ledvina and Brecht, submitted). With the better chemistry we embarked on longer runs and found something very unusual. Initially many thought, including ourselves, that the majority of the ion pickup occurred in the direction of the convection electric field.

As the simulations were run for longer times, it was noted that a majority of the pickup was occurring where the convection electric field would nominally point into the planet, thus driving ionospheric ions toward the planet. Closer examination of the electric fields showed that on the hemisphere where the convection electric field would point into the planet there were in fact parallel electric fields pointing tailward. Fig. 2 shows a plot of the $\boldsymbol{E}\cdot\boldsymbol{B}$ normalized so that 1 is perfectly aligned and −1 is anti-aligned. The plane includes the convection electric field and the Sun–Mars line. One sees that strongest parallel field pointing away from Mars on the night side in the "southern hemisphere" where crustal fields are most prevalent based on nominal solar wind IMF orientation (the magnetic field is primarily in the equatorial plane). It is also where electron precipitation into the dipole crustal fields is thought to cause aurora on Mars (Lundin et al., 2006a,b,c). One can also see presence of waves in the system possessing parallel electric fields. The left side of Fig. 2 is the "southern hemisphere" with the convection electric pointing toward the right side of the figure. The parallel electric field region coincides with the location of a large region of pickup ionospheric ions (see Fig. 5; Brain et al., submitted for publication). This suggests that the parallel electric

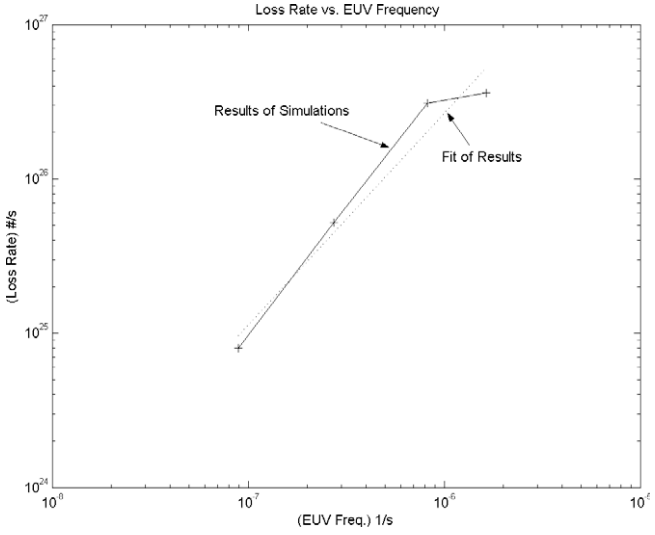

Fig. 1. The solid line is the loss rate results versus EUV freq. plotted in Log–Log. The dashed line is a crude functional fit of ion loss rate to EUV frequency using the data shown in Table 3.

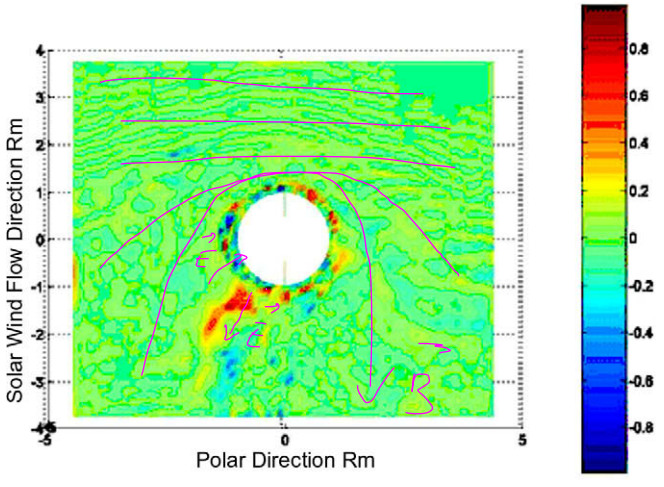

Fig. 2. Solar wind is coming from the top. Convection electric field is pointing left to right. There is a 56° Parker spiral in the simulation. The quantity plotted is $\boldsymbol{E}\cdot\boldsymbol{B}/(|B||E|)$ so that +1 has the fields parallel, and −1 is antiparallel.

field is being created by the ∇P_e term in the electric field equation. However, these parallel electric fields are time dependent. It was found that the parallel fields are not as strong in the SWIM simulation. The only difference is the neutral atmosphere profiles and the EUV flux leading to a lower density upper ionosphere. This suggests that the parallel fields are occurring due to interaction with the ionosphere (this is the only change in the simulations) and this interaction is governed by the tensor conductivity model in the code. These are speculations at this point in the research. What is required are more simulations, more time resolution with regard to the data analysis, and higher resolution of the simulations. This is in fact one of the future goals of the ongoing research.

Further, testing indicated that the parallel electric fields seen in red in the tail had magnitudes of 2–5% of the solar wind convection electric field. This translates to an electric field 2.4×10^{-5} – 6.0×10^{-5} V/m (8.0×10^{-10} – 2×10^{-9} statvolts/cm). Examining the parallel electric field region one can estimate that it is roughly 1 R_m in length providing a potential drop of roughly 82–200 V.

Both the MGS data and the MEX data have revealed the presence of aurora (Brain et al., 2006; Halekas et al., 2008; Bertaux et al., 2005; Lundin et al., 2006a,b,c; LeBlanc et al., 2006a,b, 2008). While many of the papers discuss the distribution of the auroral emissions a few discuss the electron energy spectrum (cf. Brain et al., 2006; Lundin et al., 2006a; Lundin et al., 2006a,b). It was found by these authors that energies of 100 eV to perhaps 4 keV are common in the precipitating electrons. In fact, spectra in shown in Lundin et al., 2006a show a peak at 200 eV. This suggests that the parallel fields seen in the simulations are in fact consistent with the data measured by various instruments. Are these results "iron clad"? No, much more research is going to be required to characterize the simulation results and tie together the cause and effect that creates them. However, it is clear that parallel electric fields offer an escape path from Mars and may explain the ions escaping at low energies from the "southern" pole of the planet.

Finally, closer to the planet one sees alternating parallel and anti parallel fields. These may be boundary issues, but they are often seen associated with waves propagating along the magnetic barrier region. Such fields are in fact the reason that pressure is converted from perpendicular to parallel in strongly anisotropic pressure regions. Such a region will be discussed in the next section.

6. Pressure

One of the parameters the simulators were requested to provide for code comparisons was the pressure along the Sun–Mars line to a distance beyond the shock. It seemed a reasonable request until the idea was given some thought. It was not that the comparison was unreasonable but it did opened up some very interesting questions. In this section, some of those questions will be discussed as it illustrates both the complexity of code comparisons and some of the issues raised by the simulation efforts themselves. Much of those comparisons are presented in Brain et al. (submitted for publication).

The request for pressures included thermal, magnetic, and dynamic pressures. The thermal pressure request led to some further thought. For the MHD simulations, this ended the discussion because all of the fluid codes assume a scalar pressure. Some have multiple fluids but obtaining the pressure is straight forward for Ma et al. (2004) because they actually advect pressure rather than total energy in the region around the planet. For the others it becomes a matter of parsing the internal energy between kinetic thus leaving thermal. However, for the hybrid codes the issues become a bit more complex. Do they want the pressure tensor? That is computationally available, if one takes the appropriate moments of the particle distribution functions. If one wants a scalar pressure how best to normalize the vector product? Further is the pressure tensor really diagonally dominate or are the off-diagonal terms also significant? These and other issues arose. In the following figures the thermal pressure of the incoming protons will be discussed. That of the O^+ and O_2^+ will also be addressed. These last two provided some interesting insights.

Figs. 3 and 4 show phase space plots of the hydrogen ions coming into the shock region. The solid line is the thermal velocity associated with the particle distribution. One notes in both cases that incoming (from the right) protons are reflected and then thermalized. Further there is acceleration of the particles as one can find particles exceeding ±700 km/s rather than the incoming 425 km/s. The reflected ions can be seen upstream of the shock at around 1.6–2. R_m for the SWIM simulation, Fig. 3. The reflection is seen by realizing that there are locations that have ions flowing in both directions at the same locations semi-coherent streams. It

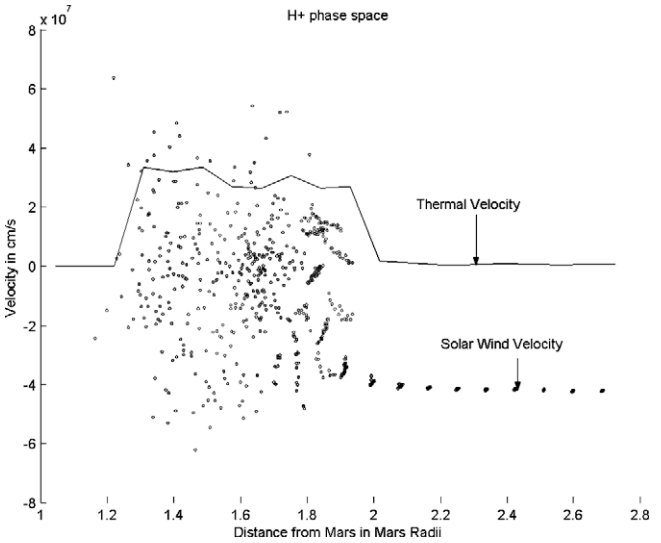

Fig. 3. The solid line is the nominal thermal velocity of the protons. The points are the particle locations and velocity in the Sun–Mars direction. The negative velocity is coming from the sun. This is from the SWIM run case.

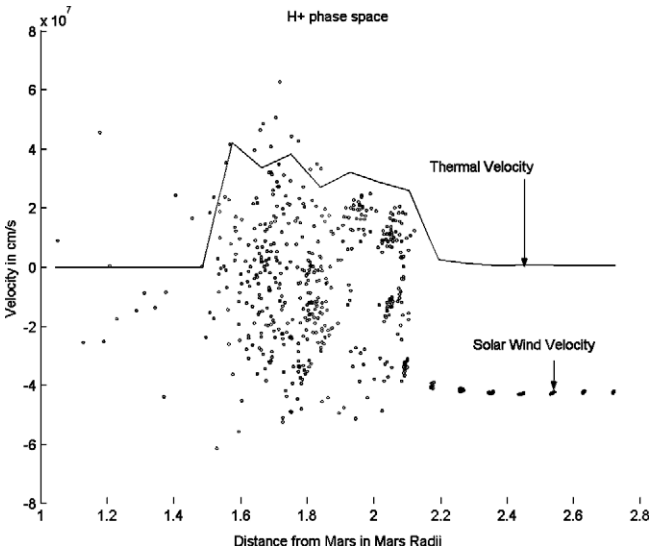

Fig. 4. The solid line is the nominal thermal velocity of the protons. The points are the particle locations and velocity in the Sun–Mars direction. The negative velocity is coming from the sun. This is from the solar maximum case associated with Phobos-2 conditions.

is should be noted that the only velocity plotted is the component aligned along the Sun–Mars line.

For the solar max. simulation, Fig. 4, one sees that the reflected ions are further out and so is the H^+ heating region in the shock. This change is directly related to the increased production associated with a high EUV flux for the solar maximum situation. Several features can be discerned from these plots. They are made at exactly the same time for both simulations. The increased EUV flux has a significant effect on both the location and thickness of the "shock" region. This is due to more efficient reflection off the shock, and some numerical issues within the chemistry package. These numerical issues will be discussed in Ledvina and Brecht (submitted). Nevertheless, the shock region is much thicker than would be found in MHD simulations because of the necessity of ion reflection and the subsequent thermalization of the incoming protons by the electromagnetic waves in the shock region. It will be shown later that the thermalization of the protons is not 100%.

In Figs. 5 and 6 one sees the various elements of the diagonal of the pressure tensor for H^+, specifically the solar wind protons. The + symbol is the pressure in the Sun–Mars direction. The ♢ symbol is the pressure in the equatorial plane. And the □ symbol is the pressure in the polar direction. Since these are "snap shots" in time one finds that the components are not balanced and will change with time as the proton population gyrates around the magnetic field lines. The black dashed line is scalar tensor created with the following formula:

$$P_{\text{scalar}} = [(P_{xx} * P_{xx} + P_{yy} * P_{yy} + P_{zz} * P_{zz})/3]^{1/2}$$

The factor 1/3 is used to normalize the distribution. One easily sees from these figures that the pressure is not a scalar. Worse, investigation of the off-diagonal elements shows that they can be as large as the diagonal elements. However, if one considers that rather than write the pressure in terms of the Sun–Mars coordinates one rotated the matrix into a coordinate system that has diagonal elements aligned and orthogonal to the magnetic field which has a 56° angle, then the elements will be diagonally dominate. However, for this paper the Sun–Mars diagonal elements will be presented.

Comparison between the nominal case (solar maximum) and the SWIM case with its smaller neutral density profile and lower EUV flux reveals some interesting features. Because of the time dependent behavior of the profiles one should exercise caution in

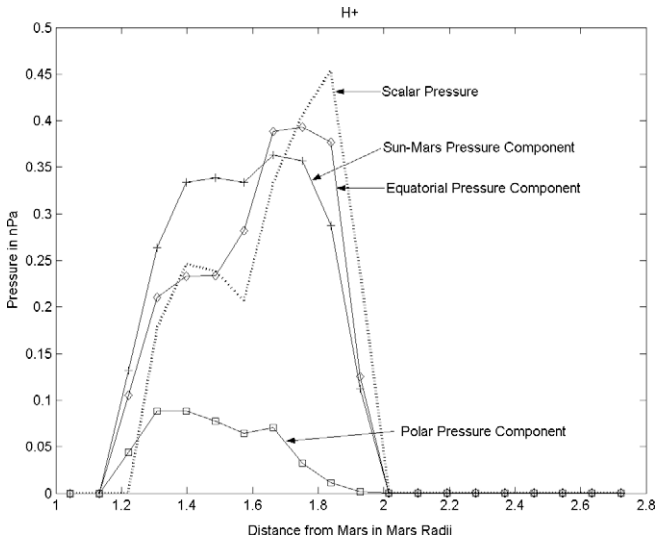

Fig. 5. The diagonal of the proton pressure tensor. The dashed line is a mean scalar pressure. This is the SWIM case. The diagonal components plotted are along the Sun-Mars line, in the equatorial plane, and perpendicular to these two vectors in the "polar" direction.

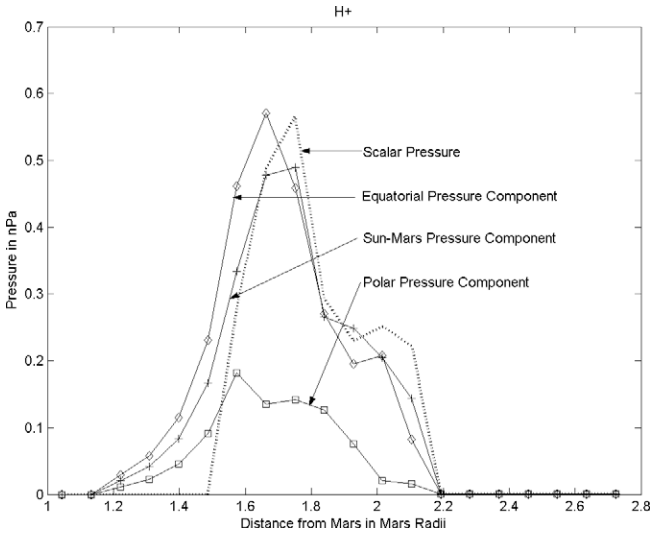

Fig. 6. The diagonal elements of the proton pressure tensor. The dashed line is the mean scalar pressure. This is the solar maximum case.

examining the details. Yet it is clear that the solar maximum case has pressure profiles extending further out than the SWIM case. However, even with this further extent the peak in the scalar proton pressure sits in roughly the same location, $1.8R_m$.

The other feature seen in Figs. 5 and 6 is the presence of waves. These waves are driven by the pressure anisotropy created by the reflected ions. These plots of pressure components illustrate that indeed the Mars system is very kinetic and not well represented by the assumption of a scalar pressure, which actually eliminates the possibility of many electromagnetic waves. However, it also illustrates something else. It illustrates why it is difficult to obtain particle distributions and measure pressure near Mars experimentally. The system is not symmetric even with regard to pressures. Further the distributions are not necessarily Maxwellian but will have tails at least.

Some very interesting issues were encountered when examining the pressure tensors for the O^+ and O_2^+. Since these simulations were performed with 250 km cell sizes and the pickup altitudes were in the range of 250–300 km in altitude, when determining the pressures for O^+ and O_2^+ a problem was encountered. The pickup by the electric field meant that some of the sampling cells had streaming ions and as well as thermal ions. Recall that our chemistry was performed on 50 km cells and because the particles are Lagrangian (they move without regard to a grid), they can be loaded anywhere we like. So when attempting to compute a thermal velocity for the O^+ and O_2^+ we were constantly obtaining velocities of 2–4 km/s which leads to pressures of ~20 nPa or greater. This issue was discussed and it was decided to apply the same assumption for the thermal velocity, as the MHD simulators did. We would assume that the electron temperature was equal to the ion temperature, $T_e \sim T_i$, using the electron temperatures in the lowest cells of data accumulation for the thermal velocity. This produced values close to the MHD codes. In the Fig. 7 one sees the O^+ and O_2^+ plots with the black dashed line being the mean of all of the pressures as computed by the formula for the scalar pressure discussed earlier. The $T_e \sim T_i$ assumption was used in computing the pressures for Fig. 7. One also notes that the pressures of the oxygen ions, O^+ and O_2^+, are isotropic, all three components of pressure are plotted. This isotropic behavior is simply a product of our assumptions when creating these terms. It is worth noting that within the ionosphere, the typical number of particles per cell is roughly 10,000 per cell. In the shock region the proton particles are usually 16–20 per cell.

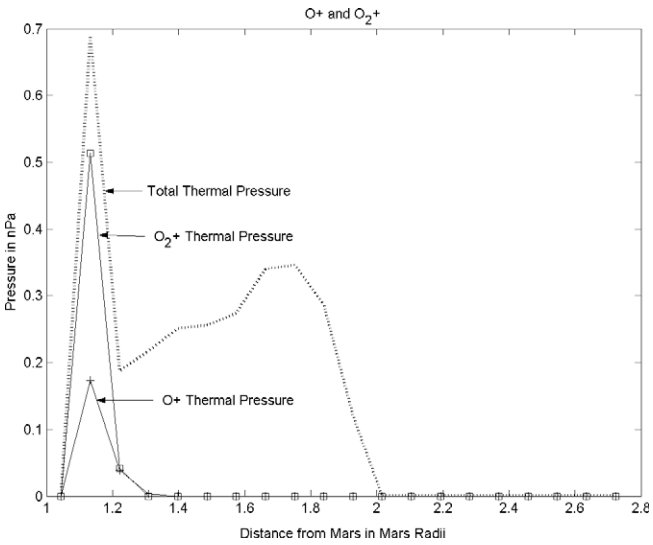

Fig. 7. Oxygen ion pressure tensor using the equal temperature assumption, $T_e \sim T_i$. The dashed line is the combined scalar pressure. The other lines (+) is the O^+ profile and (□) is the O_2^+ profile.

Fig. 7 is for the SWIM simulation situation. One sees a thicker pressure region (O^+ and O_2^+) for the solar maximum cases. Thus, the shock is pushed out further. It should be noted that the densities measured in these simulations are consistent with profiles expected at the median altitudes 100 km up. However, the thickness of the oxygen ion region is thought to be too thick although pickup is taking place.

There is another aspect of these comparisons which needs to be illustrated and that is the time dependent behavior of the subsolar region. In the following plots, Fig. 8a–c, the ram pressure (using only the velocity on the Mars–Sun line), the scalar thermal pressure, and the magnetic field pressure are plotted. They are plotted for times 1 s apart. Fig. 8a corresponds in time to Fig. 5 while Fig. 8b corresponds in time to Fig. 7.

Fig. 8c appears to most closely resemble the pressure plots shown by Brain et al. (submitted for publication). However, it is the data in Fig. 8a which was given to him. Examining these plots one sees considerable variation in some basic quantities. The ram pressure which is constructed of the velocity along the Sun–Mars line remains the same until about $2R_m$. From this point inward one can see substantial variation in the shock and reflected ion regions, $1.5R_m$ to $2R_m$. Some of the spikes seen in the ram pressure in the shock and ion reflection region are due to local counter streaming of the reflected ions and is very time dependent. Further, the ram pressure is seen to extend to altitudes of $1.2R_m$ and at one point, Fig. 8c, all the way to inner boundary of the simulation. This results strongly suggests that the shock does not completely thermalized the solar wind protons as efficiently as one would obtain in a fluid description of the interaction.

Examination of the magnetic field pressure shows considerable variation as well. Since the pressure at the shock jump is considerably smaller than the pressure scales plotted on Fig. 8a–c, one does not notice many features of the magnetic field pressure until one reaches the barrier region, which on these plots is between $1.2R_m$ and about $1.4R_m$. The peak of the magnetic pile up boundary is found to be around $1.3R_m$. However, the peak value changes by roughly 30–40% in the 2-s time span; less than 0.15 nPa to just under 0.2 nPa.

The thermal pressure is also very time dependent and spatially varying. This is not surprising given kinetic behavior of the shock interaction region, see Figs. 3 and 5. One also notes that pressure does not seem to be a constant. This is due in part to streaming

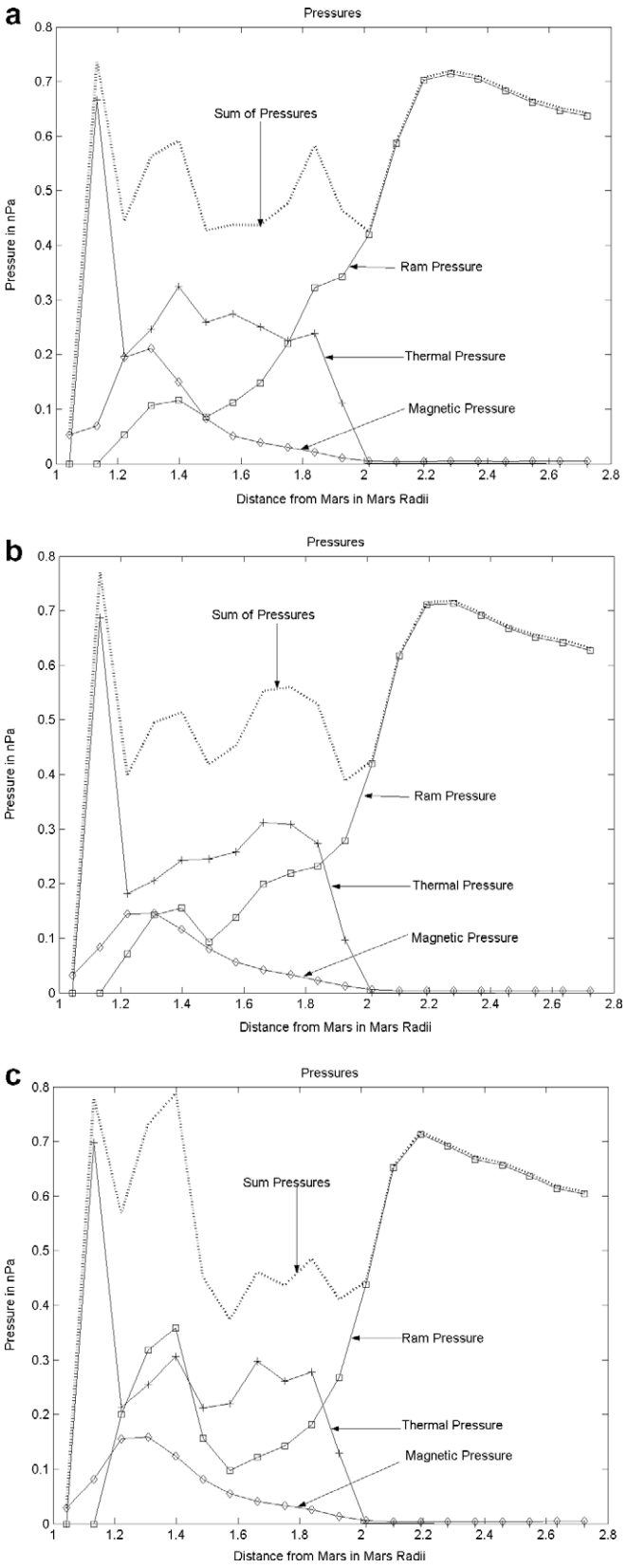

Fig. 8. (a) Pressure components along the Sun–Mars line. The dashed line is the sum of the scalar pressures for all species. Plotted are the ram pressure, the thermal pressure, and the magnetic pressure; (b) The same quantities 1 s after Fig. 8a; (c) The same quantities 2 s after Fig. 8a.

of the H^+ in directions other than the Sun–Mars directions, and to the fact that the scalar pressure constructed is not revealing

the true peaks in pressure found when examining the actual pressure tensor and its components. The off-diagonal elements of the pressure tensor have not been included in this presentation of the data and yet they are comparable to the diagonal components. Examining Fig. 8a and b, and comparing the region where H^+ pressure is dominate, Fig. 5, one sees that the "drop out" region in the "sum of pressures" curve ($1.3–2R_m$) is where the off-diagonal pressure elements are largest. The level of the drop as compared to the incoming solar wind ram pressure provides a rough estimate of how much pressure is contained in the off-diagonal components.

These issues and the temporal/spatial variations makes it very clear that code comparison and even comparison to data are very difficult. It further illustrates the difficulty one encounters when analyzing the data. A detail comparison would require all parties to decide on what elements of the pressure to compare and in what coordinate system, Sun–Mars, or magnetic where $P_\perp$ and $P_\square$ are then the orthogonal components. It also suggests that the hybrid results need to be time-averaged over at least the inverse cyclotron frequency if not the proton ion gyro-period when comparing to the MHD results.

7. Shock location

One of the more interesting things that was compared at the Chapman conference was the shock location. While it is of interest, it has not been a point of major interest for our research. Why? The shock on Mars has been shown to be extremely variable. This is in fact due to the electromagnetic wave nature of the shock (Vignes et al., 2000; Trotignon et al., 2006; Mazelle et al., 2004; Brecht and Ferrante, 1991). However, it is interesting to note that even within the parameters specified for the Chapman conference or not specified as the case may be there is a variation of the shock. It was noted that the shock location provided for the comparison was further out than the nominal shock envelop provided by data averages. Other simulations seemed to match better. The MHD codes must provide a fluid result, symmetrical in all regions and smooth. The hybrid codes provided varying results and a lot of that was based on planetary boundary conditions. But, more interestingly was that some groups included the mass loading created by the EUV ionization of the neutral corona surrounding Mars in their simulations and others such as ours Brain et al. (submitted for publication) did not.

It was decided to make an additional run with the ionized component of the neutral corona in the simulation. The results can be seen in Fig. 9a and b which show the shock location in the same format as in Brain et al. (submitted for publication). In Fig. 9a one sees the shock location without the additional ionization. In Fig. 9b one sees the shock at the same time step as before with the contribution from the ionized neutral corona included in the simulation. The additional ionization produces a noticeable movement of the shock location and one that makes it fit better into the envelop especially on the flanks. The purpose of this comparison is to point out that adding this small additional source of ionization (mass loading) changes the wave characteristics around the planet, and since the shock is formed and structured by electromagnetic waves and ion reflection, changing the characteristics changes the shock shape. So when examining details or performing code comparisons, at least within the hybrid code groups even the neutral corona must be specified, something no one had thought to do before the comparison.

8. Discussion

The SWIM comparison was an excellent idea and has led to some interesting insights into the simulation state of the art and what it will take to compare to the data. The realization that the distribution functions are often not Maxwellian and the pressure is a tensor versus the scalar assumption illustrates some of the underlying issues with the data collection and interpretation itself. Nevertheless, the comparisons have led the authors to rethink our diagnostics and some of the simulations that need to be performed. It has also illustrated areas of sensitivity and those requiring further specification for a more comprehensive comparison with other codes, much less with the data.

The exercise in computing the pressure in the sub-solar direction also illustrated that although the particle loading algorithm allows us to load at any resolution desired. The field and the data analysis grid resolution needs significant improvement in resolution. Given what was been shown, the resolution of the grid needs to have a 50 km radial resolution. As discussed in Ledvina and Brecht (submitted), the chemistry resolution had to be improved to cells of less than 20 km, and probably around 10 km. This has been completed and tested as was shown in the afore mentioned paper. Further, work involving collecting the pressures and such will need to use the more sophisticated allocation schemes used in the code itself, thus reducing noise.

One of the more interesting aspects of the research reported was the presence of parallel fields. They are not strong but may well explain some of the auroral data taken in recent Mars missions. However, the location of these parallel fields leads naturally to the issue of addressing the crustal fields. The presence of the crustal fields clearly has the potential to change the ion pickup rates from Mars. There are at least three magnetic field models presently being used. They are by Purucker et al. (2000), Arkani-Hamed (2001), and Cain et al. (2003). Fig. 10 shows the 100 nT surface from the Purucker model. It clearly shows the rather mottled structure of the field surfaces and the fact that orientation with respect to the solar wind will probably be a parameter to be addressed. In Fig. 10 one is seeing the crustal fields from the direction of the sun. It is clear that in the region (southern hemisphere/bottom) where slow ion pick up is occurring due to parallel electric fields there exists many of the strongest crustal fields as

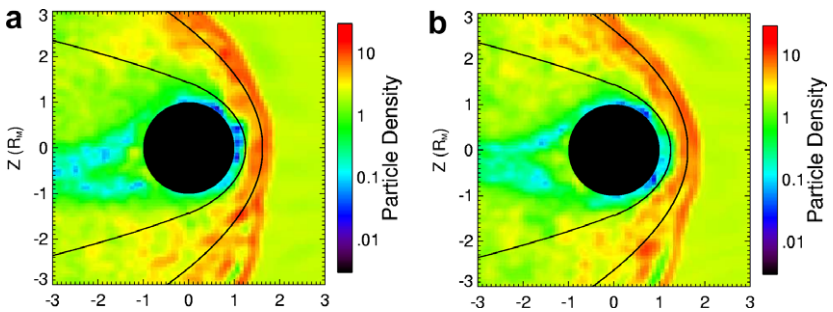

Fig. 9. (a) Shock envelop with no ionization of the neutral corona in the simulation. (b) Shock envelop with ionization of the neutral corona in the simulation.

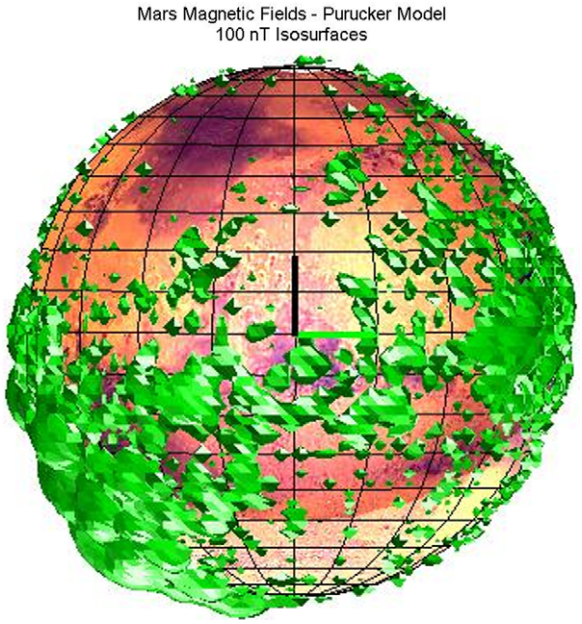

Fig. 10. Using the Purucker magnetic field model the 100 nT surface levels of the crustal fields on Mars are plotted.

well as the most strongly clustered sites of crustal fields. The location of the slow ion pickup will change as the IMF is changed, as it is the convection electric field that defines "poles" for the purposes of ion pickup, not the frozen regions on the planet.

The crustal fields present a major computational challenge to kinetic codes because the ion gyrofrequency increases linearly with magnetic field and the spatial resolution must go down to continue to resolve the ion gyroradius. Following the placement and resolution of an ionosphere in the codes, the next challenge is the inclusion of these fields. It is expected that the results that have been obtained so far will be modified by the presence of the crustal fields.

9. Summary

The hybrid particle simulations performed for the code comparisons and as a continuation of our research show Mars to be very sensitive to changes in input conditions, boundary conditions (both numerical and physical, the neutral profiles for example). It is yet to be determined if core pieces of information such as the global loss rate are in fact as sensitive given that somewhat differing numerical approaches produce similar answers. However, as the simulation tools are refined and known weakness addressed the sensitivities with regard to important issues will be discovered. Therefore code comparisons as well as comparisons with data are crucial to the evolution of our knowledge about Mars.

The detection of parallel electric fields was a surprise. It is interesting to note that estimated magnitudes and associated potential drops seems consistent with estimates and energies associated with auroral data taken to date. It is also worth recalling that these structures are temporally and spatially varying. Further, research needs to be undertaken to address these features in light of higher resolution of the electromagnetic grid as well as the chemistry grid.

The future of the present research includes increasing the numerical resolution by factors of at least 6. It will focus on the parallel electric fields that seem to play a role in the pick up of ions on the side opposite the convection electric field. With the new resolution the roll of crustal fields in the ion loss and solar wind interaction will be revisited.

This paper has shown the kinetic behavior of the interaction, but it also illustrated where considerably more work needs to be performed in order for these simulations to reach the level of fidelity necessary to make definitive statements about Mars' interaction with the solar wind in the past, now, and in the future. It was also the goal of this paper to illustrate that comparisons with functional dependencies is in our mind crucial. Finally, it is still not clear if ion pickup can explain the loss of water from Mars. However, the loss rates measured for the simulations at EUV fluxes higher than solar maximum suggest ion pickup is a viable mechanism. More research needs to be undertaken to place reasonable levels of uncertainty on the results of the simulations to date. Further code comparisons should accomplish this task.

Acknowledgments

The authors of this paper would like to thank Dr. David Brain for very useful discussions and his efforts to organize the SWIM conference. The author's research was supported by NASA contract NNH06CC05C.

References

Acuna, M., and 19 colleagues, 1998. Magnetic field and plasma observations at Mars: Initial results of the Mars Global Surveyor mission. Science 279, 1676–1680.
Arkani-Hamed, Jafar, 2001. A 50-degree spherical harmonic model of the magnetic field of Mars. J. Geophys. Res. 106, 23197–23208.
Bertaux, J.-L., Leblanc, F., Witasse, O., Quemerais, E., Lilensten, J., Stern, S.A., Sandel, B., Korablev, O., 2005. Discovery of an aurora on Mars. Nature Lett. 435, 790–794.
Bößwetter, A., Bagdonat, T., Motschmann, U., Sauer, K., 2004. Plasma boundaries at Mars: A 3D simulation study. Ann. Geophys. 22, 4363–4397.
Brain, D.A., Halekas, J.S., Petcolas, L.M., Lin, R.P., Luhmann, J.G., Mitchell, D.L., Delory, G.T., Bougher, S.W., Acuña, M.H., Rème, H., 2006. On the origin of aurorae on Mars. Geophys. Res. Lett. 33. doi:10.1029/2005GL024782.
Brain, D., Barabash, S., Böesswetter, A., Bougher, S., Brecht, S.H., Chanteur, G., Crider, D., Dubinin, E., Fang, X., Fraenz, M., Halekas, J., Harnett, E., Holmstrom, M., Kallio, E., Lammer, H., Ledvina, S.A., Liemohn, M., Liu, K., Luhmann, J.G., Ma, Y., Modolo, R., Mötschmann, U., Nagy, H., Nilsson, H., Shinagawa, N. Terada. (submitted for publication). First results from the SWIM model challenge. Icarus.
Brecht, S.H., 1990. Magnetic asymmetry of unmagnetized planets. Geophys. Res. Lett. 17, 1243–1246.
Brecht, S.H., 1995. Shock formation at unmagnetized planets. In: Russell, C.T. (Ed.), COSPAR Adv. in Space Research: Physics of Collisionless Shocks, vol. 15, p. 415–421.
Brecht, S.H., 1995b. Consideration of the Martian magnetotail as evidence for an intrinsic magnetic field. Geophys. Res. Lett. 22, 1181–1184.
Brecht, S.H., 1997a. Solar wind proton deposition into the Martian Atmosphere. J. Geophys. Res. 102, 11287–11294.
Brecht, S.H., 1997b. Hybrid simulations of the magnetic topology of Mars. J. Geophys. Res. 102, 4743–4750.
Brecht, S.H., Ferrante, J.R., 1991. Global hybrid simulation of unmagnetized planets: Comparison of Venus and Mars. J. Geophys. Res. 96, 11209–11220.
Brecht, S.H., Ledvina, S.A., 2006. The solar wind interaction with the Martian Ionosphere/Atmosphere. Space Sci. Rev. 126, 15–38.
Brecht, S.H., Thomas, V.A., 1988. Multidimensional simulations using hybrid particle codes. Comp. Phys. Comm. 48, 135–143.
Brecht, S.H., Ferrrante, J.R., Luhmann, J.G., 1993a. Three-dimensional simulations of the solar wind interaction with Mars. J. Geophys. Res. 98, 1345–1357.
Brecht, S.H., Luhmann, J.G., Larson, D.J., 2000. Simulations of the Saturnian magnetospheric interaction with Titan. J. Geophys. Res. 105, 13119–13130.
Cravens, T.E., Kozyra, J.U., Nagy, A.F., Gombosi, T.I., Kurtz, M., 1987. Electron impact ionization in the vicinity of comets. J. Geophys. Res. 92, 7341–7353.
Cain, Joseph C., Ferguson, Bruce B., David, Mozzoni, 2003. An $n = 90$ internal potential function of the Martian crustal magnetic field. J. Geophys. Res. (Planets) 108. doi:10.1029/2000JE001487.
Fox, J.L., 1997. Upper limits to the outflow of ions at Mars: Implications for atmospheric evolution. Geophys. Res. Lett. 24, 2901.
Halekas, J.S., Brain, D.A., Lin, R.P., Luhmann, J.G., Mitchell, D.L., 2008. Distribution and variability of accelerated electrons at Mars. Adv. Space Res. 41, 1347.
Harned, D.S., 1982. J. Comp. Phys. 47, 452–462.
Harnett, E.M., Winglee, R.M., 2006. Three-dimensional multifluid simulations of ionospheric loss at Mars from nominal solar wind conditions to magnetic cloud events. J. Geophys. Res. 111. doi:10.1029/2006JA011724.
Kallio, E., Janhunen, P., 2002. Ion escape from Mars in a quasi-neutral hybrid model. J. Geophys. Res. 107. doi:10.1029/2001JA000090.
Lammer, H., Stumptner, W., Bauer, S.J., 1996. Loss of H and O from Mars: Implications for the planetary water inventory. Geophys. Res. Lett. 23, 3353–3356.

Lammer, H., Lichtennegger, H.I.M., Kolb, C., Ribas, I., Guinan, E.F., Abart, R., Bauer, S.J., 2003. Loss of water from Mars: Implications for the oxidation of the soil. Icarus 165, 9–25.

LeBlanc, F., Witasse, O., Winningham, J., Brain, D., Lilensten, J., Blelly, P.-L., Frahm, R.A., Haledas, J.S., Bertaux, J.L., 2006a. Origins of the Martian aurora observed by the Spectroscopy for Investigation of characteristics of the atmosphere of Mars (SPICAM) on board Mars Express. J. Geophys. Res. 111. doi:10.1029/2006JA001763.

Leblanc, F., Chaufray, J.Y., Lilensten, J., Witasse, O., Bertaux, J.-L., 2006b. Martian dayglow as seen by the SPICAM UV spectrograph on Mars Express. J. Geophys. Res. 111, E09S11. doi:10.1029/2005JE002664.

Leblanc, F., Witasse, O., Lilensten, J., Frahm, R.A., Safaenili, A., Brain, D.A., Mouginot, J., Nilsson, H., Futaana, Y., Halekas, J., Holmström, M., Bertaux, J.L., Winningham, J.D., Kofman, W., Lundin, R., 2008. Observations of aurorae by SPICAM ultraviolet spectrograph on board Mars Express: Simulataneous ASPERA-3 and MARSIS measurements. J. Geophys. Res. 113, A08311. doi:10.1029/2008JA013033.

Ledvina, S.A., Brecht, S.H. (submitted for publication). A basic Martian ionospheric model: Assumption, properties and 3D hybrid implementation strategy. Icarus.

Ledvina, S.A., Brecht, S.H., Luhmann, J.G., 2004. Ion distributions of 14 AMU pickup ions associated with Titan's plasma interaction. Geophys. Res. Lett. 31, L17S10.

Ledvina, S.A., Ma, Y.-j., Kallio, E., 2008. Modeling and simulatingflowing plasmas and related phenomena. Space Sci. Rev. 139, 143–189.

Liu, Y., Nagy, A.F., Gombosi, T.I., DeZeeuw, D.L., Powell, K.G., 2001. The solar wind interaction with Mars: Results of the three-dimensional three species MHD studies. Adv. Space Res. 27, 2689–2692.

Lundin, R., Zakharov, A., Pellinen, R., Hultquist, B., Borg, H., Dubinin, E.M., Barabash, S.W., Pissarenko, N., Koskinen, H., Liede, I., 1989. First results of the ionospheric plasma escape from Mars. Nature 341, 609–612.

Lundin, R., Zakharov, A., Pellinen, R., Barabash, S.W., Borg, H., Dubinin, E.M., Hultquist, B., Koskinen, H., Liede, I., Pissarenko, N., 1990. ASPERA/Phobos measurements of the ion outflow from the Martian ionosphere. Geophys. Res. Lett. 17, 873–876.

Lundin, R., Winningham, D., Barabash, S., Frahm, R., Anderson, H., Holmström, M., Grigoriev, A., Yamauchi, M., Borg, H., Sharber, J.R., Sauvaud, J.-A., Fedorov, A., Fedorov, A., Thocaven, J.-J., Asamura, K., Hayakawa, H., Coates, A.J., Linder, D.R., Kataria, D.O., Curtis, C., Hsieh, K.C., Sandel, B.R.K.C., Grande, M., Carter, M., Reading, D.H., Koskinen, H., Kallio, E., Riihelä, P., Schmidt, W., Säles, T., Kozyra, J., Krupp, N., Woch, J., Fränz, M., Luhmann, J., McKenna-Lawler, S., Cerulli-Irelli, R., Orsini, S., Maggi, M., Roelof, E., Williams, D., Livi, S., Brandt, P., Wurz, P., Bochsler, P., 2006a. Ionospheric plasma acceleration at Mars: ASPERA-3 results. Icuras 182, 308–310.

Lundin, R., Winningham, D., Barabash, S., Frahm, R.A., Holmström, M., Sauvaud, J.-A., Fedorov, A., Asamura, K., Coates, A.J., Soobiah, Y., Hsieh, K.C., Grande, M., Koskinen, H., Kallio, E., Kozyra, J., Woch, J., Fraenz, M., Brain, D., Luhmann, J., McKenna-Lawler, Orsini, S., Brandt, P., Wurz, P., 2006b. Auroral plasma acceleration above martian magnetic anomalies. Science 311, 980–983.

Lundin, R., Winningham, D., Barabash, S., Frahm, R., Brain, D., Nilsson, H., Holmström, M., Yamauchi, M., Sharber, J.R., Sauvaud, J.-A., Fedorov, A., Asamura, K., Hayakawa, H., Coates, A.J., Soobiah, Y., Curtis, C., Hsieh, K.C., Grande, M., Koskinen, H., Kallio, E., Kozyra, J., Woch, J., Fraenz, M., Luhmann, J., McKenna-Lawler, S., Orsini, S., Brandt, P., Wurz, P., 2006c. Auroral plasma acceleration above martian magnetic anomalies. Space Sci. Rev. 126, 333–354.

Lundin, R., Barabash, S., Holmstrom, M., Nilsson, H., Ymauchi, M., Fraenz, M., Dubinin, E.M., 2008. A comet-like escape of ionospheric plasma from Mars. Geophys. Res. Lett. 35. doi:10.1029/GL034811.

Ma, Y.A., Nagy, A.F., Hansen, K.C., DeZeeuw, D.L., 2002. Three-dimensional multispecies MHD studies of the solar wind interaction with Mars in the presence of crustal fields. J. Geophys. Res. 107, 1282. doi:10.1029/2002JA009293.

Ma, Y., Nagy, A.F., Sokolov, I.V., Hansen, K.C., 2004. Three-dimensional, multispecies, high spatial resolution MHD studies of the solar wind interaction with Mars. J. Geophys. Res. 109. 1029/2003JA010367.

Mazelle, C., Winterhalter, D., Sauer, K., Trotignon, J.G., Acuña, M.H., Baumgärtel, K., Bertucci, C., Brain, D.A., Brecht, S.H., Delva, M., Dubinin, E., Øierset, M., Slavin, J., 2004. Bow shock and upstream phenomena at Mars. Space Sci. Rev. 111, 115–181.

Mitchner, M., Kruger Jr., C.H., 1973. Partially Ionized Gases. Wiley, New York, USA.

Modolo, R., Chanteur, G.M., Dubinin, E., Matthews, A.P., 2005. Influence of the solar EUV flux on the Martian plasma environment. Ann. Geophys. 23, 433–444.

Nagy, A.F., Winterhalter, D., Sauer, K., Cravens, T.E., Brecht, S.H., Mazelle, C., Crider, D., Kallio, E., Zakharov, A., Dubinin, E., Verigin, M., Kotova, G., Axford, W.I., Bertucci, C., Trotignon, J.G., 2004. The plasma environment of Mars. Space Sci. Rev. 111, 33–114.

Purucker, M., Ravat, D., Frey, H., Voorhies, C., Sabaka, T., Acuña, M., 2000. An altitude-normalized magnetic map of Mars and its interpretation. Geophys. Res. Lett. 27, 2449–2452.

Shinagawa, H., Cravens, T.E., 1989. A one-dimensional mult-species magnetohydrodynamic model of the dayside ionosphere of Mars. J. Geophys. Res. 94, 6506–6516.

Strangeway, R., 1996. Collisional joule dissiapation in the ionosphere of Venus, the importance of electron heat conduction. J. Geophys. Res. 101, 2279–2296.

Trotignon, J.G., Mazelle, C., Bertucci, C., Acuña, M.H., 2006. Martian shock and magnetic pile-up boundary positions and shapes determined from the Phobos 2 and Mars Global Surveyor data sets. Planet. Space Sci. 54, 357–369. doi:10.1016/j.pss.2006.01.003.

Vignes, D., Mazelle, C., Reme, H., Acuna, M.H., Connnerney, J.E.P., Lin, R.P., Mitchell, D.L., Cloutier, P., Crider, D.H., Ness, N.F., 2000. The Solar Wind interaction with Mars: Locations and shapes of the Bow Shock and the Magnetic Pile-up Boundary from the observations of the MAG/ER experiment onboard Mars Global Surveyor. Geophys. Res. Lett. 27, 49–52.